ADVANCED FUNCTIONAL MATERIALS

Photoswitchable Spirobenzopyran-Based Photochemically Controlled Photonic Crystals**

By *Marta Kamenjicki Maurer*, *Igor K. Lednev*, and *Sanford A. Asher**

We have developed a photochemically controlled photonic-crystal material by covalently attaching spiropyran derivatives to polymerized crystalline colloidal arrays (PCCAs). These PCCAs consist of colloidal particles that self-assemble into crystalline colloidal arrays (CCAs), which are embedded in crosslinked hydrogels. Photoresponsive PCCAs were made two ways: 1) by functionalizing the hydrogel network with spiropyran derivatives, and 2) by functionalizing the colloidal particles with spiropyran derivatives. These materials can diffract light in the UV, visible, or near-IR spectral regions. The diffraction of the PCCAs is red-shifted by exciting the spiropyran with UV light. Alternatively, the diffraction is blue-shifted by exciting the spiropyran with visible irradiation. Thus, this material acts as a memory storage material where information is recorded by illuminating the PCCA and information is read out by measuring the photonic-crystal diffraction wavelength. UV excitation forms the open spiropyran form while visible excitation forms the closed spiropyran form. The diffraction shifts result from changes in the free energy of mixing of the PCCA system as the spiropyran is photoexcited to its different stable forms.

1. Introduction

There is intense interest in fabricating materials with photonic bandgaps in the visible, infrared, and microwave spectral regions.[1,2] The idea is to develop materials which can be used as light waveguides, where light is used for processing information. The simplest method for producing materials with photonic bandgaps involves the use of crystalline colloidal array (CCA) self assembly where monodisperse, highly charged, nano- and mesoscale colloidal particles form cubic arrays (Fig. 1).[3] These particles are generally negatively charged due to the ionization of surface strong-acid groups. The electrostatic repulsive interactions result in the formation of face-centered cubic (fcc) arrays where the particles are spaced by distances significantly larger than their diameters. The periodic spacings diffract the light and form bandgaps at the angles that fulfil the Bragg condition.[3–5]

Our group developed methods to polymerize hydrogels around the highly plastic CCA to form more robust solid materials called polymerized crystalline colloidal arrays (PCCAs, Fig. 1).[6,7] These PCCAs contain the periodic array that gives rise to the photonic bandgap. A major advantage of PCCAs is that they can be further chemically modified to make them responsive to their chemical, thermal, and photonic environments.[8–12] For example, we prepared chemical sensors where the photonic bandgap shifts in frequency in response to changing analyte concentrations.[8,9] We also developed a thermally responsive PCCA where poly-*N*-isopropylacrylamide (PNIPAM) was used for the hydrogel. This PNIPAM shows a temperature-driven volume phase transition such that the photonic bandgap wavelength can be tuned throughout the visible spectral region by varying the temperature between 10–40 °C.[11] In addition, we recently demonstrated a photoresponsive azobenzene-based PCCA,[12] where the photochemistry of the azobenzene derivative was used to drive shifts in the bandgap diffraction wavelength upon excitation with UV and visible light.

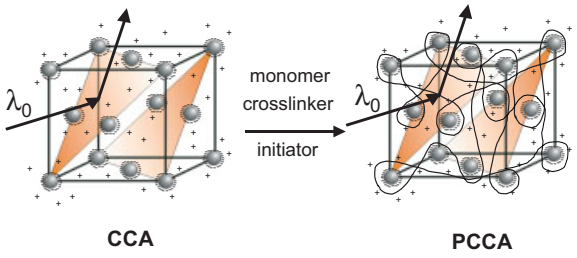

Figure 1. Synthesis of a polymerized crystalline colloidal array (PCCA).

In this work, we demonstrate a second example of a photochemically actuated PCCA in which photoisomerization of a covalently attached spirobenzopyran modulates the PCCA's bandgap. Photoisomerization of a PCCA with a covalently attached spirobenzopyran chromophore changes the hydrogel's free energy of mixing due to the large change in charge distribution within the spirobenzopyran molecule.[13] The resulting PCCA volume change alters the CCA lattice constant and shifts the bandgap and the diffracted wavelength.

[*] Prof. S. A. Asher
Department of Chemistry, University of Pittsburgh
Pittsburgh, PA 15260 (USA)
E-mail: asher@pitt.edu
Prof. M. Kamenjicki Maurer
Department of Chemistry, Pennsylvania State University–Altoona
Altoona, PA 16601 (USA)
Dr. I. K. Lednev
Department of Chemistry, University of Albany, SUNY
Albany, NY 12222 (USA)

[**] This work was supported by an NSF NIRT grant and NASA/NCI Contract (N01-CO-17016-32).

 DOI: 10.1002/adfm.200400070

2. Results and Discussion

2.1. PCCAs with Spirobenzopyran Linked to the Hydrogel

Figure 2a shows the molecular structural changes that occur for spirobenzopyran as it photochemically cycles from its spiropyran (closed) form to its merocyanine (open) form. Figure 2b shows that for spirobenzopyran in dimethylsulfoxide (DMSO) the merocyanine form has a visible absorption band at ~560 nm, whereas the spiropyran form mainly absorbs light in the UV region. Intense UV illumination converts the majority of the spiropyran form to the merocyanine form, resulting in a photostationary state (PSS-UV, Fig. 2b). In contrast, intense visible illumination converts a majority of the spirobenzopyran molecules to their spiropyran form; the ~560 nm absorption band decreases, and the system stabilizes in a photostationary state (PSS-Vis, Fig. 2b).

The dashed line in Figure 3a shows the extinction spectrum of the photoresponsive PCCA containing spirobenzopyran linked to the hydrogel network, just after saturating excitation by UV light (mercury lamp, 365 nm, 40 mW cm^{-2}). In contrast, the solid line in Figure 3a shows the extinction spectrum after saturating excitation with visible light (tungsten lamp, 500–750 nm, 40 mW cm^{-2}). UV excitation converts spirobenzopyran from its spiropyran to merocyanine form, which increases the ~350 and ~560 nm absorption in a manner similar to that for spirobenzopyran monomer in solution (Fig. 2). However, the absorption increase at 350 nm is much greater for the PCCA–spirobenzopyran sample than for spirobenzopyran monomer in solution (compare Fig. 3. to Fig. 2).

The PCCA in the DMSO medium was oriented such that the light was incident normal to the fcc (111) planes (glancing angle, $\theta = 90°$), resulting in diffraction of ~680 nm light (λ_{diff}) after saturating UV excitation (Fig. 3a). Under these conditions, and with a PCCA refractive index $n \sim 1.48$, the spacing between the (111) planes, d_{111}, is calculated to be 220 nm from Braggs law ($n\lambda_{diff} = 2d_{111}\sin\theta$). Figure 3 also shows that the UV photostationary state PSS-UV 680 nm diffraction peak blue-shifts by 13 nm upon saturation with visible excitation (PSS-Vis). Since little change can occur in the refractive index at these low spiropyran concentrations, the diffraction shifts must arise from volume changes in the PCCA. The 13 nm change represents a 2.5 % shrinkage in the linear dimension, which if isotropic, would arise from a >7 % volume shrinkage of the PCCA upon illumination with visible light.

As discussed below, the hydrogel-linked spirobenzopyran samples relax in the dark over periods of days to a dark equilibrium state (DES), which has an absorption spectrum essentially identical to that of the PSS-Vis state shown in Figure 3. The inset of Figure 3a shows the relative magnitude of the absorption at 550 nm for the DES, PSS-Vis, and PSS-UV states. The DES of spirobenzopyran monomers (Fig. 2) has a significantly larger 550 nm absorption than occurs for the hydrogel-linked PCCA (Fig. 3). Part of the absorption differences in the 280–330 nm region between Figure 2 and Figure 3 results from the overlapping absorption of the polystyrene particles. It should be noted that previous studies demonstrated that changes in solvent, pH, and metal binding can greatly influence the spirobenzopyran absorption spectra.[14–19]

Figure 3b shows the results of an experiment in which we excited our sample with 355 nm UV excitation (yttrium aluminum garnet (YAG) laser, 20 mW cm^{-2}) and 514.5 nm visible excitation (Ar^+ laser, 20 mW cm^{-2}) and monitored the changes in the diffraction wavelength. 514.5 nm excitation of the PSS-UV state results in a ~11 nm diffraction blue-shift and formation of the PSS-Vis state over a characteristic time of ~25 min at these intensities. Subsequent UV excitation red-shifts the diffraction ~10 nm over a similar timescale, and forms the PSS-UV state.

These diffraction shifts probably derive from differences in the charge distribution and resulting dipole moments between the open and closed forms of spirobenzopyran. UV photoisomerization to the

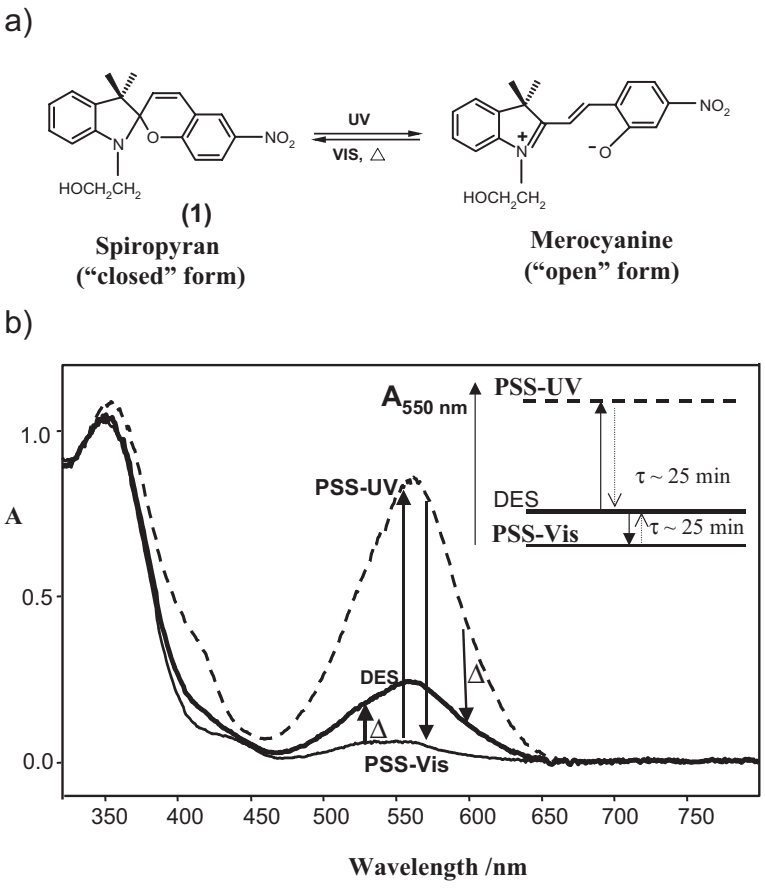

Figure 2. a) Molecular structural change for the spirobenzopyran photochemical interconversion from its closed to open form. b) Photochemistry of spirobenzopyran (**1**) in DMSO. PSS-UV and PSS-Vis are the photostationary states under UV and visible light irradiation, respectively; Inset: shows 550 nm absorption of photostationary and dark equilibrium state (DES) under UV and visible irradiation (40 mW cm^{-2}). 1 mm quartz cell, concentration = 4×10^{-4} M.

ADVANCED FUNCTIONAL MATERIALS

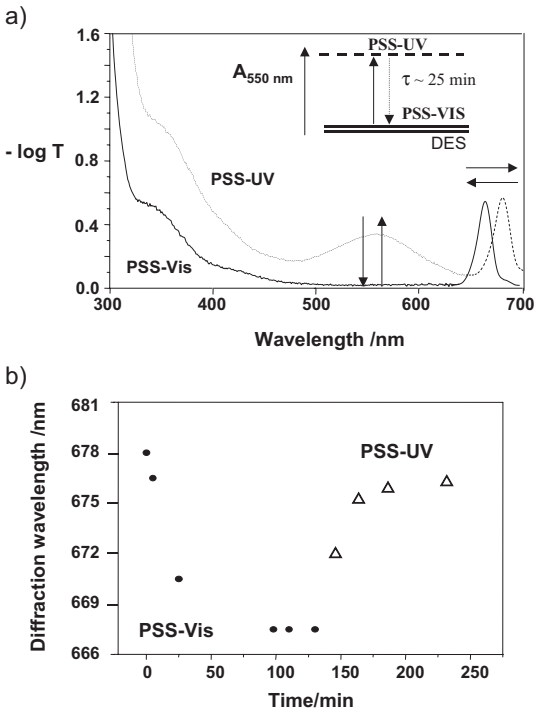

Figure 3. a) Extinction spectra of 80 μm PCCA with spirobenzopyran (~5 mM) linked to hydrogel under UV (mercury lamp, ~25 min, 40 mW cm^{-2}) and visible irradiation (tungsten lamp, ~25 min, 40 mW cm^{-2}). b) Photoswitching behavior of the PCCA. The system was exposed to 514 nm light (Ar^+ laser, 20 mW cm^{-2}) and 355 nm (YAG, 20 mW cm^{-2}).

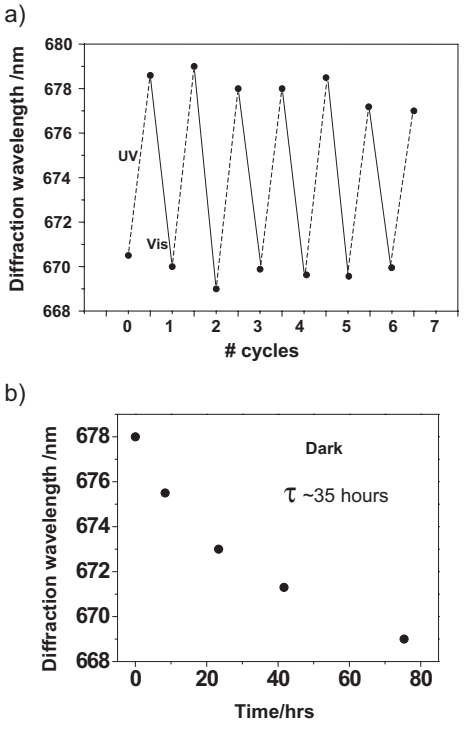

Figure 4. a) Photoswitching behavior of the PCCA at 25 °C with spirobenzopyran linked to the hydrogel. The system was exposed to alternating irradiation with a YAG laser (355 nm, 20 mW cm^{-2}) and a Ar^+ laser (514 nm, 20 mW cm^{-2}). b) Thermal relaxation at 25 °C (starting from PSS-UV).

open, merocyanine form results in formation of a zwitterion, which results in a more favorable free energy of mixing of the hydrogel with the DMSO medium. This causes a swelling of the hydrogel resulting in the diffraction red-shift. We previously[12] demonstrated a somewhat similar phenomenon for an azobenzene-derivatized PCCA. In contrast, visible irradiation blue-shifts the diffraction due to formation of the spirobenzopyran closed form, which reduces the dipole moment and shrinks the PCCA (Fig. 3b).

Figure 4a shows that the diffraction of our system can be toggled indefinitely by alternating irradiation with UV and visible light. The system shows ~10 nm diffraction peak red-shifts and blue-shifts upon alternative irradiation with UV light (20 mW cm^{-2}) and visible light (20 mW cm^{-2}). We left the PCCA stabilized in PSS-UV state in the dark and monitored the time dependence of diffraction. We found that the characteristic dark thermal recovery time of the PCCA to the DES state at 25 °C is ~35 h (Fig. 4b). We observe photochemical degradation for these samples at temperatures significantly greater than 25 °C.

2.2. PCCAs with Spiropyran Linked to Colloidal Particles

The photochemistry of spirobenzopyran derivatives depends strongly on their detailed chemical structure and their environment.[20] Spiropyran derivatives can display either "positive" photochromic behavior, where the DES state only weakly absorbs visible light, or "negative" photochromic behavior, where the DES shows strong visible absorption.[20] UV wavelength excitation increases the absorption of positive photochromics, but decreases it for the negative photochromics.

Since spirobenzopyrans with low visible absorptions are generally in their closed forms, we expect that positive photochromic behavior involves a transition from the closed to the open form of spiropyran. In contrast, negative photochromics should involve transitions from an open form to a closed form.[21]

The black line in Figure 5a shows the DES extinction spectrum of a 40 μm thick PCCA made from spirobenzopyran-linked poly(styrene chloromethylstyrene) colloidal particles. In addition to a poly(styrene chloromethylstyrene) particle absorption (~280–330 nm), we observe very broad spirobenzopyran UV (~330–450 nm) and visible absorption (~500–600 nm) bands. Upon UV irradiation (mercury lamp, 365 nm, ~10 min exposure, 40 mW cm^{-2}), the DES ~650 nm diffraction peak blue-shifts 5 nm, stabilizing in the PSS-UV state (Fig. 5, blue line). Additional irradiation of this PSS-UV state with visible light causes an additional 9 nm diffraction blue-shift (PSS-Vis, Fig. 5, red line). Starting from the DES and applying visible (rather than UV) light results in the same PSS-Vis state, with a 14 nm diffraction blue-shift. Exciting the PSS-Vis state with UV light red-shifts the diffraction 9 nm (Fig. 5b).

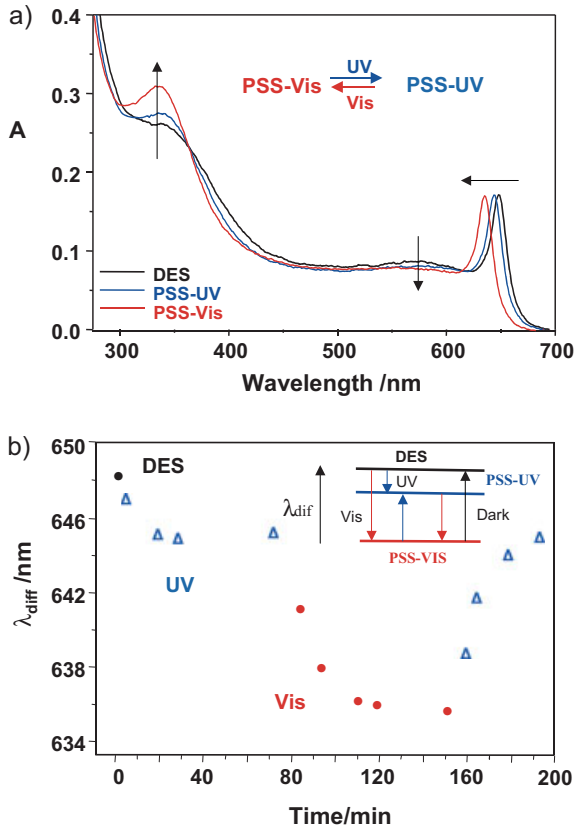

Figure 5. a) Extinction spectra of 40 μm thick PCCA functionalized with spirobenzopyran derivative linked to the colloidal particles in DMSO. b) Changes in the diffraction peak over time under UV and visible irradiation. PSS-UV and PSS-Vis are the photostationary states under UV and visible light, respectively.

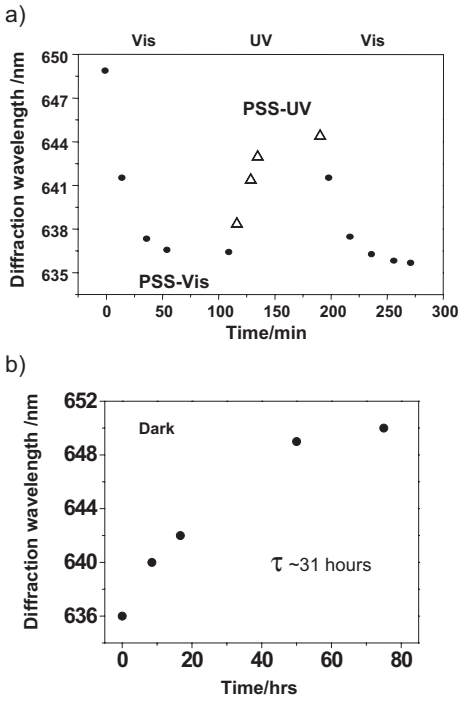

Figure 6. a) Irradiation of PCCA with spirobenzopyran linked to colloidal particles with visible (Ar^+ laser, 514 nm line, 20 mW cm^{-2}) and UV (YAG laser, 355 nm line, 20 mW cm^{-2}) light. b) Dark relaxation at 25 °C (starting from PSS-Vis).

While we observe changes in the diffraction wavelength upon excitation with visible and UV light, we see little change in the extremely broad visible absorbance. In addition, the visible absorption of the DES state is essentially identical to the PSS-UV and PSS-Vis states. This behavior dramatically differs from that of the PCCA discussed earlier with the spirobenzopyran linked to the hydrogel, in which a red-shift in the diffraction always occurs with UV irradiation, a blue-shift occurs with visible irradiation (Fig. 4a), and significant absorption spectral changes occur at ~560 and ~350 nm (Fig. 3a).

We do not understand the photochemical behavior of the spiropyran-linked particles in detail. The DES shows the most red-shifted diffraction, which suggests dominating presence of the open merocyanine form, which has a more favorable free energy of mixing due to its higher dipole moment. This system can be excited by UV light to a state which is blue-shifted from the DES by 5 nm, with a further 9 nm blue-shift caused by excitation with visible light (Fig. 5b). Subsequently, the diffraction can be toggled back and forth 14 nm with alternating UV and visible excitation (Fig. 6a). This suggests that the concentration of the closed form in the PSS-UV is between the closed spiropyran-dominated PSS-Vis and the open merocyanine-dominated DES.

The different forms of spiropyran in this sample appear to have similar absorbances in the visible region. This may result from additional chemistry that occurs for the spiropyran derivatives bound to the particles, compared to those bound to the PCCA hydrogel. For example, Salhin and co-workers, and Reichardt reported that metal ion interactions with the phenolate anion on the merocyanine form of spirobenzopyran can induce "negative" photochromism.[18,22,23] In addition, Shimizu et al.[24] and Zhou and co-workers[25] showed that in the presence of acid, the open form may steadily transform into the protonated form ($pK_a = 3.93$), which is also negatively photochromic. Since the pH around the sulfonated colloidal particles is ~3, it is possible that the merocyanine form in the PCCA with spirobenzopyran linked to colloidal particles is completely converted to (or coexists with) the protonated form. Irradiation with visible or UV light causes formation of the closed form, and dark relaxation results in the opposite process. Despite the different photochemistry in this system, the thermal dark relaxation time (30–35 h, Figs. 4b,6b) and the characteristic photoswitching time between the PSS-Vis and PSS-UV states (~20 min, Figs. 3,5) are essentially identical to those of the PCCA with spirobenzopyran linked to the hydrogel.

3. Conclusions

The change of spirobenzopyran molecules from the closed to open form causes a PCCA diffraction wavelength red-shift due to the change in charge localization of the attached spirobenzo-

ADVANCED FUNCTIONAL MATERIALS

pyran. The higher charge localization makes the hydrogel network (in the first system) and the colloidal particles (in the second system) more soluble in DMSO, causing an increase in the free energy of mixing of the PCCA. This causes swelling of the hydrogel, and red-shifts the PCCA diffraction wavelength.

The system described here could be utilized for slow switching applications (seconds to minutes) such as optical memory devices. The kinetics of gel swelling and shrinking depends on the driving osmotic pressure associated with changes in the free energy of mixing balanced by the collective diffusion constant of the polymer network relative to the solvent.[26–28] The swelling and shrinkage times should scale approximately with the hydrogel length-scale.[29,30] For macroscopic gels the times are on the order of seconds to minutes.

4. Experimental

4.1. Synthesis of Photoresponsive Hydrogel-Linked Spirobenzopyran PCCAs

Spirobenzopyran-containing PCCAs were fabricated by covalently attaching a spirobenzopyran derivative to the hydrogel network. We accomplished this by reacting *N*-(*p*-maleimidophenyl)isocyanate (PMPI, Pierce), a sulfohydryl-reactive and hydroxyl-reactive heterobifunctional crosslinker [31], with a spirobenzopyran derivative containing a hydroxyl group (Fig. 7). The isocyanate end of PMPI reacts with the hydroxyl groups on the spirobenzopyran, forming urethane linkages. This product contains maleimide ends, which, when coupled to a thiol-containing PCCA, forms stable thioether linkages (Fig. 7) [31,32].

The HS-PCCA was made by dissolving 5 mg of *N,N′*-cystamine-bisacrylamide (Aldrich), 50 mg acrylamide, 3 mg *N,N′*-methylenebisacrylamide (Sigma) and 10 μL diethoxyacetophenone (DEAP) in 1 g of a 10 wt.-% polystyrene CCA dispersion. This dispersion was injected into a cell made of two quartz plates separated by a 80 μm thick spacer (DuraSeal) and exposed to UV light (Black Ray model B-100, UVP Inc. mercury lamp). After 30 min irradiation, the cell was opened and the gel was removed and washed with NanoPure deionized water. Exposing this PCCA (3 cm × 3 cm × 80 μm) to an aqueous solution of dithiolthreitol (DTT, ACROS Organics) cleaved the disulfide bonds to leave reactive thiol groups within the PCCA [32]. During this process, the hydrogel swelled due to the breaking of crosslinks, and the diffraction wavelength red-shifted 40 nm to 590 nm. This 80 μm thick PCCA was then incubated with a 6 mM solution of maleimide-functionalized spirobenzopyran in DMSO for two hours at room temperature. From absorption measurements we calculate that we have a 5 mM concentration of spirobenzopyran within the PCCA.

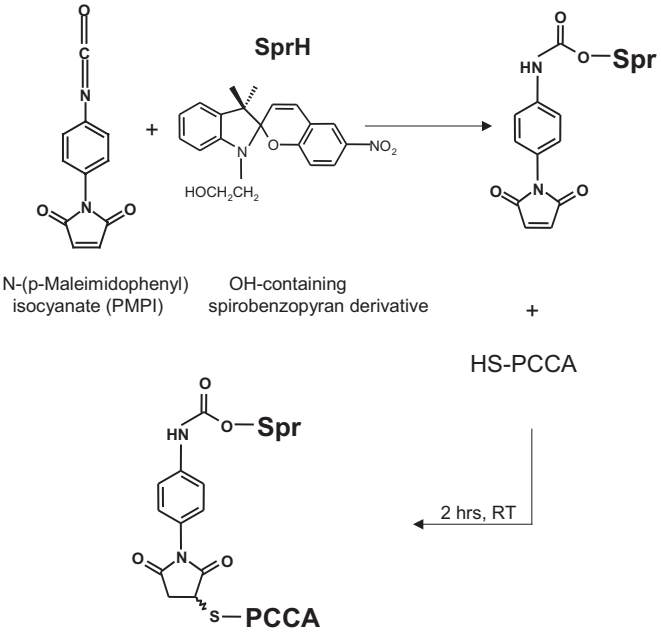

Figure 7. Reaction between hydroxylated spirobenzopyran (SprH) and PMPI, and subsequent functionalization of the sulfhydryl-containing PCCA with maleimide-containing spirobenzopyran.

4.2. Synthesis of Photoresponsive Spirobenzopyran-Linked Colloidal Particle PCCAs

4.2.1. Synthesis of Chloromethyl-Functionalized Polystyrene Particles

Chloromethyl-functionalized polystyrene particles were synthesized by emulsion polymerization by using a 10 wt.-% suspension of previously synthesized 120 nm polystyrene colloidal particles as seed particles [33]. These highly charged, monodisperse polystyrene colloidal particles were prepared via emulsion polymerization, as described elsewhere [34].

In a 500 mL jacketed reaction flask, 76 g of the 10 wt.-% seed polystyrene colloid dispersion and 15 mL of NanoPure water were purged with nitrogen for 20 min. 0.04 mol of styrene (Aldrich) and 0.03 mol of chloromethylstyrene (ACROS Organics) were added to the reaction flask, and the mixture was stirred at 200 rpm at 30 °C under nitrogen. The seed particles were allowed to swell for one hour. The reaction temperature was raised to 60 °C, and the initiator, consisting of 0.17 g potassium persulfate (Aldrich) and 0.12 g sodium bisulfite (JT Baker) in 5 mL NanoPure water, was added. After 4 h, the resulting crude poly(styrene chloromethylstyrene) core–shell colloidal particle dispersion was removed from the reaction vessel and dialyzed against NanoPure water for one week (until the conductivity of the dialysate was 1.0 $\mu\Omega^{-1}\,cm^{-1}$). A transmission electron microscopy image of the synthesized colloids demonstrated that these were core–shell particles. The colloidal suspension was further cleaned by shaking the suspension with a mixed bed ion-exchange resin (Bio-Rad AG 501-X8), after which it became iridescent due to Bragg diffraction (460 nm at normal incidence) from the 135 nm diameter poly(styrene chloromethylstyrene) CCA. Elemental microanalysis of these particles showed 3 % chlorine by weight.

4.2.2. Synthesis of Spiropyran-Linked Colloidal Particle PCCAs

A mixture of 50 mg acrylamide (Sigma), 3 mg *N,N′*-methylenebisacrylamide (Sigma), 10 μL DEAP (Aldrich), and 1 g of a 10 wt.-% dispersion of 135 nm poly(styrene chloromethylstyrene) CCA, was injected into a cell made of two quartz plates separated by a 40 μm spacer, and exposed to UV light (Black-Ray model B-100 A, UVP Inc.) for 1 h. The 3 cm × 3 cm × 40 μm gel was then removed from the cell, washed with NanoPure water, and gradually transferred to a pure DMSO medium. The PCCA was then exposed to 15 mL of a 6 mM DMSO solution of 1-(2-hydroxyethyl)-3,3-dimethyl-6′-nitrospiro(indoline-2,2′-[2*H*-1] benzopyran) (Chroma Chemicals, Fig. 2a) for 2 days at room temperature, in the dark. This spirobenzopyran derivative contains a hydroxyl group, which can undergo a nucleophilic substitution reaction by the chlorines on the polystyrene colloidal particle surfaces. After 2 days of incubation, we utilized absorption spectroscopy to determine that the spirobenzopyran concentration in the PCCA was 2.5 mM, indicating that all the spirobenzopyran attached to the colloidal particles. During this procedure the hydrogel swelled and diffraction wavelength red-shifted to 650 nm. No attachment of spirobenzopyran occurred in a control experiment where the PCCA was prepared only with pure polystyrene colloidal particles.

In order to measure the photochemical response, we irradiated the PCCA in DMSO with UV light (Black Ray model B-100, UVP Inc. mercury lamp, 365 nm maximum wavelength) and visible light (CUDA Products Corp., Model 1-150 tungsten lamp with a UV rejection filter; wavelength range between 500–750 nm). In addition, we measured the kinetics of the diffraction change in the seconds time range using a YAG (355 nm) and an Ar^+ laser (514.5 nm).

Received: February 20, 2004
Final version: February 24, 2005
Published online: August 2, 2005

[1] J. D. Joannopoulos, R. D. Meade, J. N. Winn, *Photonic Crystals: Molding the Flow of Light*, Princeton University Press, Princeton, NJ **1995**.

[2] a) T. F. Krauss, R. M. De La Rue, *Prog. Quantum Electron.* **1999**, *23*, 51. b) G. A. Ozin, S. M. Yang, *Adv. Funct. Mater.* **2001**, *11*, 95. c) P. Jiang, G. N. Ostojic, R. Narat, D. M. Mittleman, V. L. Colvin, *Adv. Mater.* **2001**, *13*, 389. d) D. J. Norris, Y. A. Vlasov, *Adv. Mater.* **2001**, *13*, 371.

[3] a) I. M. Krieger, F. M. O'Neil, *J. Am. Chem. Soc.* **1968**, *90*, 3114. b) P. A. Hiltner, H. S. Papir, I. M. Krieger, *J. Phys. Chem.* **1971**, *75*, 1881. c) N. A. Clark, A. J. Hurd, B. J. Ackerson, *Nature* **1979**, *281*, 57. d) P. Pieranski, *Contemp. Phys.* **1983**, *24*, 25.

[4] a) S. A. Asher, *US Patent 4 627 689*, **1986**. b) S. A. Asher, *US Patent 4 632 517*, **1986**. c) S. A. Asher, P. L. Flaugh, G. Washinger, *Spectroscopy* **1986**, *1*, 26. d) R. J. Carlson, S. A. Asher, *Appl. Spectrosc.* **1984**, *38*, 297. e) P. L. Flaugh, S. E. O'Donnell, S. A. Asher, *Appl. Spectrosc.* **1984**, *38*, 847.

[5] a) R. Kesavamorthy, S. Jagannathan, P. A. Rundquist, S. A. Asher, *J. Chem. Phys.* **1991**, *94*, 5172. b) P. A. Rundquist, R. Kasavamoorthy, S. Jagannathan, S. A. Asher, *J. Chem. Phys.* **1991**, *95*, 1249. c) S. A. Asher, J. M. Weissman, A. Tikhonov, R. D. Coalson, R. Kesavamoorthy, *Phys. Rev. E* **2004**, *69*, 066 619.

[6] a) G. Haacke, H. P. Panzer, L. G. Magliocco, S. A. Asher, *US Patent 5 266 238*, **1993**. b) S. A. Asher, S. Jagannathan, *US Patent 5 281 370*, **1994**. c) S. A. Asher, J. M. Weissman, H. B. Sunkara, G. Pan, J. Holtz, L. Liu, R. Kasavamoorthy, in *Polymers for Advanced Optical Applications* (Eds: S. A. Jenekhe, K. J. Wynne), Washington, DC **1997**.

[7] S. A. Asher, J. Holtz, L. Liu, Z. Wu, *J. Am. Chem. Soc.* **1994**, *116*, 4997.

[8] a) J. H. Holtz, S. A. Asher, *Nature* **1997**, *389*, 829. b) J. H. Holtz, J. S. W. Holtz, C. H. Munro, S. A. Asher, *Anal. Chem.* **1998**, *70*, 780. c) S. A. Asher, S. Peteu, C. Reese, M. Lin, D. Finegold, *Anal. Bioanal. Chem.* **2002**, *373*, 632.

[9] S. A. Asher, V. L. Alexeev, A. V. Goponenko, A. C. Sharma, I. K. Lednev, C. S. Wilcox, D. N. Finegold, *J. Am. Chem. Soc.* **2003**, *125*, 3322.

[10] K. Lee, S. A. Asher, *J. Am. Chem. Soc.* **2000**, *122*, 9534.

[11] a) J. M. Weissman, H. B. Sunkara, A. S. Tse, S. A. Asher, *Science* **1996**, *274*, 959. b) C. Reese, A. Mikhonin, M. Kamenjicki, A. Tikhonov, S. A. Asher, *J. Am. Chem. Soc.* **2004**, *126*, 1493.

[12] a) S. A. Asher, M. Kamenjicki, I. Lednev, *US Patent 6 589 452*, **2003**. b) M. Kamenjicki, I. Lednev, A. Mikhonin, R. Kasavamoorthy, S. A. Asher, *Adv. Funct. Mater.* **2003**, *13*, 774.

[13] M. Blets, U. Pfeifer-Fukumura, U. Kolb, W. Baumann, *J. Phys. Chem. A* **2002**, *106*, 2232.

[14] P. Uznanski, *Langmuir* **2003**, *19*, 1919.

[15] a) R. C. Bertelson, *Techniques of Chemistry*, Vol. 3 (Ed: G. H. Brown), Wiley-Interscience, New York **1971**, 45. b) J. Zhou, Y. Li, Y. Tang, F. Zhao, X. Song, E. Li, *J. Photochem. Photobiol. A* **1995**, *90*, 117.

[16] H. Tachibana, Y. Yamanaka, M. Matsumoto, *J. Phys. Chem. B* **2001**, *105*, 10 282.

[17] C. B. McArdle, H. Blair, A. Barraud, A. Ruaudel-Teixier, *Thin Solid Films* **1983**, *99*, 181.

[18] M. Tanaka, M. Nakamura, A. M. A. Salhin, T. Ikeda, K. Kamada, H. Ando, Y. Shibutani, K. Kimura, *J. Org. Chem.* **2001**, *66*, 1533.

[19] M. Tanaka, T. Ikeda, Q. Xu, H. Ando, Y. Shibutani, M. Nakamura, H. Sakamoto, S. Yajima, K. Kimura, *J. Org. Chem.* **2002**, *67*, 2223.

[20] a) M. J. Kamlet, J. L. Abboud, R. W. Taft, *J. Am. Chem. Soc.* **1977**, *99*, 6027. b) C. Bohne, M. C. Fan, Z. J. Li, Y. C. Liang, J. Lusztyk, J. C. Scaiano, *J. Photochem. Photobiol. A* **1992**, *66*, 79. c) K. Kimura, T. Yamashita, M. Yokoyama, *J. Chem. Soc., Chem. Commun.* **1991**, 147.

[21] A. A. Garcia, S. Cherian, J. Park, D. Gust, F. Jahnke, R. Rosario, *J. Phys. Chem. A* **2000**, *104*, 6103.

[22] A. M. A. Salhin, M. Tanaka, K. Kamada, H. Ando, T. Ikeda, Y. Shibutani, S. Yajima, M. Nakamura, K. Kimura, *Eur. J. Org. Chem.* **2002**, 655.

[23] C. Reichardt, *Chem. Rev.* **1994**, *94*, 2319.

[24] I. Shimizu, T. Nakayama, H. Kokado, E. Inoue, *Bull. Chem. Soc. Jpn.* **1970**, *43*, 2244.

[25] Y. Li, Y. Tang, J. Zhou, X. Song, E. Li, *J. Photochem. Photobiol. A* **1995**, *90*, 117.

[26] T. Tanaka, D. Fillmore, *J. Chem. Phys.* **1979**, *70*, 121.

[27] A. Peters, S. J. Candau, *Macromolecules* **1986**, *19*, 1952.

[28] E. S. Matsuo, T. Tanaka, *J. Chem. Phys.* **1988**, *89*, 1695.

[29] M. Tokita, K. Miyamoto, T. Komai, *J. Chem. Phys.* **2000**, *113*, 1647.

[30] T. Tanaka, L. Hocker, G. B. Benedek, *J. Chem. Phys.* **1973**, *59*, 5151.

[31] M. E. Annunziato, U. S. Patel, M. Ranade, P. S. Palumbo, *Bioconjugate Chem.* **1993**, *4*, 212.

[32] G. T. Hermanson, *Bioconjugate Techniques*, Academic Press, San Diego **1996**.

[33] a) J. Sarobe, J. Forcada, *Colloid Polym. Sci.* **1996**, *274*, 8. b) J. Park, J. Kim, K. Suh, *Colloids Surf. A* **2001**, *191*, 193. c) T. Tsoukatos, S. Pispas, N. Hadjichristicks, *Macromolecules* **2000**, *33*, 9504. d) U. Meyer, F. Svec, J. H. Frechet, *Macromolecules* **2000**, *33*, 7769. e) J. Suh, S. Oh, *J. Org. Chem.* **2000**, *65*, 7534.

[34] C. E. Reese, C. D. Guerrero, J. M. Weissman, K. Lee, S. A. Asher, *J. Colloid Interface Sci.* **2000**, *232*, 76.